Enhancement of silicon based solar cell using optimized plasmonic nanoparticles and window shape implantation

DONYA ADABI[1,*], MOHAMMAD REZA MOSLEMI[2], MOHAMMAD REZA SHAYESTEH[1],
SAEEDEH HASHEMIAN[3]
[1]Department of Electrical Engineering, Yazd Branch, Islamic Azad University, Yazd, Iran
[2]Department of Electrical Engineering, Zarghan Branch, Islamic Azad University, Zarghan, Iran
[3]Chemistry Department, Yazd Branch, Islamic Azad University, Yazd, Iran

In this study, a novel single junction silicon solar cells have been proposed for the sake of enhancing efficiency and improving current-voltage characteristics. The proposed structure has a window-shaped of doping. The structure also includes an innovative profile of plasmonic nanoparticles. It is shown that by adding nanoparticles with the proposed shape, the field strength in the active region is greatly improved and thus leads to a significant improvement in solar cell performance. For this purpose, we use spherical and elliptical plasmonic nanoparticles made of gold and silver. The number, location and material of nanoparticles as well as the number of windows of doping are optimized to achieve the highest possible solar cell performance. The simulation results showed that the EQE and light/dark current are improved noticeably using window shaped doping along with optimized plasmonic nanoparticles.

1. Introduction

Solar cells are structures that convert direct sunlight into electrical current. [1]. In fact, a solar cell is an electronic device that converts sunlight energy directly into electricity using a photovoltaic effect.

The photoelectric effect describes the discharge of positive charge carriers during a solid state when light strikes its surface. The absorbed light causes electrons within the material to extend in energy, at an equivalent time making them liberal to move around within the material. However, the electrons remain at this higher energy for less than a brief time before returning to their original lower energy position. A p-n junction is usually used for gathering the carriers before they lose the energy gained from the sunshine. The p-n junction consists of p+ and n+ semiconductor layer [1].

High efficiency photovoltaic cell design requires optically thick photovoltaic layers to enable nearly complete light absorption. For this reason, the fabric thickness normally chose several times of minority carrier diffusion lengths to permit efficient carrier collection. However, the reduced material utilization in addition to increase in cell efficiency motivate a discount in cell active region. A beautiful approach involves plasmonic nano-structures. In recent years, plasmonic nanoparticles closely coupled to absorbing semiconductors are utilized to reinforce absorption in ultrathin film solar cells [2-5].

The antenna-like response of the nanoparticles caused by the dipole oscillation of the localized surface plasmons serves to extend the tissue extinction for incident light due to an enhanced local electromagnetic field in the vicinity of the nanoparticles upon surface plasmon resonance, which also leads to an increased scattering cross section for nonresonant light. From the photovoltaic conversion point of view, the plasmonic resonance absorption is an undesirable loss process, but the enhanced scattering outside the resonance can increase the absorption and photocurrent collection. Since the optical properties of plasmonic nanoparticles depend sensitively on the size and shape of the nanoparticles, [6] a suitable morphological design of the nanoparticles can be a prerequisite for achieving highly efficient plasmonic solar cells [7]. Recently, structures that can trap light and induce strong scattering and nanophotonic modes [8-9] have demonstrated their great ability to trap light and offer tremendous opportunities for thin film solar cells. Both dielectric and metallic nanostructures are used for nanophotonic light trapping, but their functional mechanisms differ significantly. Specially designed metallic nanostructures can excite surface plasmon resonance (SPR) or surface plasmon polariton (SPP) at the metal-dielectric interface by interacting with the incident light, resulting in a highly localized and reconstructed electromagnetic field [10-11]. Plasmonic nanostructures improve the performance of photovoltaic (PV) devices by either guiding or focusing the incident light. On the other hand, lossless dielectric nanostructures improve the performance of photovoltaic cells by antireflection or photonic modes.

Among the various proposed plasmonic structures, nanoparticles are extremely advantageous for photovoltaic applications due to their strong scattering properties, which are tunable depending on the particle species, size,

shape, and dielectric environment, as well as their simple preparation and integration methods, which are readily compatible with the fabrication process for high quality photovoltaic cells without significantly increasing the assembly costs [10-25]. Metallic nanoparticles supporting localized surface plasmons (LSP) in the visible or near-infrared region can significantly improve the sunshine length in solar cells [12, 16, 26-31]. Metallic nanoparticles and nanostructures can improve the performance of optical devices like solar cells via three main mechanisms: (1) far-field effect and scattering by the metallic nanoparticle and (2) increasing the near-field of light by small nanoparticles, that directly enhance the semiconductor absorption in close proximity to the nanoparticles; (3) by coupling light into SPP modes of a nanostructured metal solar cell layer [32-35].

In recent years, rapid progress has been made in the field of plasmonic solar cells. Various methods of fabricating nanoparticles and nanostructures are being explored. So far, plasmonic effects have been studied in most types of solar cells [36-39].

Various structures for light trapping have been proposed for ultrahigh efficiency and low cost solar cells [40-42]. Among all designs, metallic nanoparticles are the only and most commonly used plasmonic nanomaterials that effectively enhance the absorption of solar cells [10-25]. These nanoparticles, which act as scatterers, are integrated on the top or back surface of the solar cells during cell fabrication [12, 16, 26-30]. Both experiments and simulations have shown that after the integration of nanoparticles, the sunshine absorption in solar cells is often improved, especially in the longer wavelength range near the band gap of the absorbers, where more light can be scattered thanks to the plasmonic enhanced scattering [16, 30, 31].

In this paper, we propose a novel profile of plasmonic nanoparticles to improve the performance of single junction silicon solar cells. Both spherical and elliptical plasmonic nanoparticles of gold and silver are used in the proposed solar cell. The number, location and material of the nanoparticles and the number of doping windows are optimized to achieve the highest possible performance of the solar cell. In addition to using plasmonic nanoparticles, we use impurity window structure to increase the absorption and trapping of more light in the solar cell. The window structure leads to more light trapping in the active region and improves the performance of the solar cell.

This paper is organized as follows. In section two, we describe the structure of the proposed solar cell. The theory of the proposed nanoparticles and the optimization method are also presented in this section. In section three, the simulation results of the proposed structure are presented. In section four, the paper is summarized. Finite-difference time-domain (FDTD) and CDA (coupled-dipole approximation) method was used for simulation of proposed solar cell structure which considers the effects of the near field enhancement. So the behavior of nanoparticles together (nanoparticles array) is considered in simulation results. The simulation method is added in revised version of manuscript. The CDA (coupled-dipole approximation) method is a powerful tool for simulating nanoparticles with alternating structures. A schematic of an alternating structure is given in Fig. 1. In this form, all nanoparticles are at the same distance from the side nanoparticles. As mentioned in the previous sections, the adsorption of nanoparticles is strongly dependent on the arrangement of nanoparticles. Therefore, alternating arrangements are expected to have better absorption. A binary CDA (BCDA) method is proposed to simulate nanoparticles with alternating structures. Using this method, the effect of adsorption on nanoparticles with different arrangements can be investigated. A major advantage of this method is its use when using evolutionary optimization algorithms.

2. The structure of MGIM waveguide

Fig. 1 shows the proposed structure of the solar cell. As can be seen in the figure, the structure consists of some window-shaped doped regions and also includes a number of symmetrically distributed nanoparticles below the impurity region. The nanoparticles increase the field strength in the active region and consequently absorb more photons and increase the efficiency and power of the solar cell, and the window-shaped regions increase the absorption of more light and absorb more. The window profile with nanoparticles leads to more confinement, more adsorption and more efficiency of the solar cell. As shown in Fig. 1, in the proposed structure, the performance of the solar cell can be optimized by changing the depth (D) and the distance between two window-shaped impurity regions (d).

In addition, a number of spherical and elliptical nanoparticles of gold or silver have been added in the center of the layer instead of alternating spherical nanoparticles. The number, shape (spherical or elliptical), and the material (gold or silver) of nanoparticle would be optimized to reach the maximum possible performance for solar cell.

As shown in Fig. 1, nanoparticles were added to the center of the proposed structure just below the windowed regions to improve the adsorption rate. The shape, location and number of these nanoparticles (the number of vacancies in the nanoparticles) are optimized using a heuristic method. The scheme of periodic and non-periodic structures is shown in Fig. 1. Fig. 2 shows some other possible non-periodic nanoparticles. In the non-periodic structure, some nanoparticles are removed or replaced with silver (shown in pink in Fig. 2). The distances between each two adjacent nanoparticles (or vacancies of nanoparticles) are equal. This figure shows a quarter of the center of the graphene layer to simplify optimization. Since the adsorption of nanoparticles strongly depends on the arrangement of nanoparticles, it is expected that optimizing the nanoparticles and the number of vacancies as well as the silver and gold can noticeably improve the performance of the solar cell.
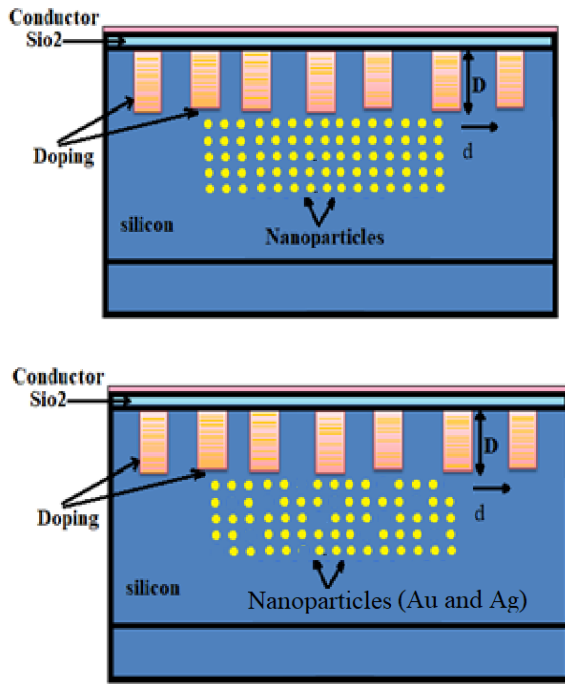
Fig. 1. Structure of the proposed solar cell under consideration
with periodic profile of nanoparticles (top) and non- periodic
profile of nanoparticles (bottom) (color onlne)
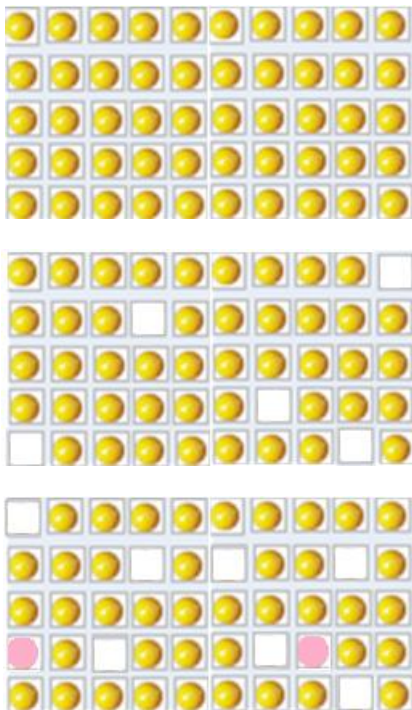
Fig. 2. An alternating and non-alternating structure of
nanoparticles (color online)

The first step in determining the best arrangement of
nanoparticles is to find the best position of each
nanoparticle and vacancies in the x, y directions. The
algorithm for positioning nanoparticles and vacancies is
shown in Fig. 3.
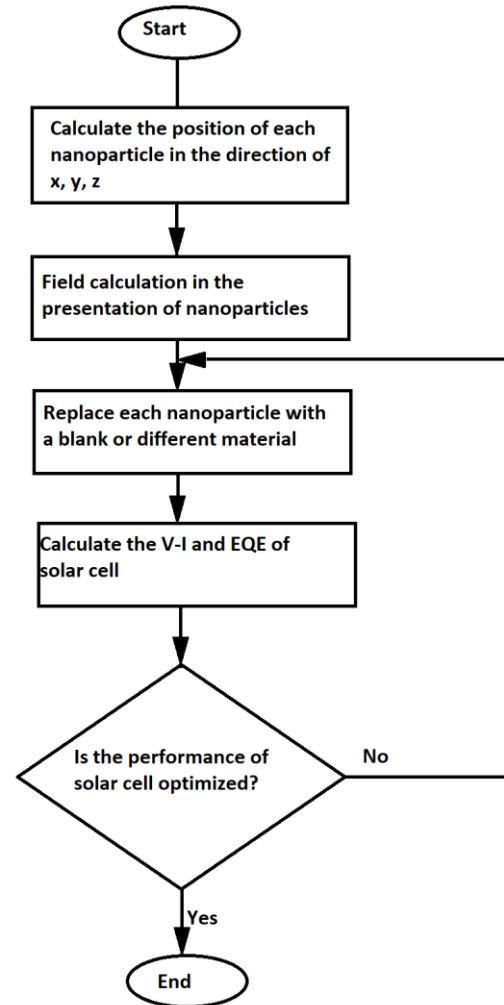
Fig. 3. Nanoparticle and vacancy positioning algorithm

In this quasi-code, r represents the position of each
nanoparticle, N1, N2, N3 are also the number of
nanoparticles in the direction x, y, z representative. D is
the distance between nanoparticles and the vector B(i, j, k)
is a binary tensor. If an element of this tensor takes the
value one, it means the presence of a particle at position (i,
j, k). If an element becomes zero, it means that the position
(i, j, k) is not occupied by a nanoparticle. In the second
step, we need to model the effect of the input field on the
nanoparticles. To do this, we assume that a plane field is
input in the desired plane:

$$\mathbf{E}_{inc}(\mathbf{r}, t) = \mathbf{E}_0\, e^{j(\mathbf{k}\mathbf{r}_s - \omega t)} \qquad (1)$$

If the incident light enters at an angle of θ,φ the field
in each nanoparticle can be viewed as follows:

$$\mathbf{E}_{inc}(\mathbf{r}_s) = \mathbf{E}_0 e^{j\mathbf{k}.\mathbf{r}_s} \qquad (2)$$

In these relations, the parameters λ r, t, ω, k = ω / c = 2π / λ, c are respectively the wavelength of the incident light, the speed of light, the wave vector, the angular frequency, the time and the location vector. In this context, the parameter k is also calculated using the following equation:

$$\mathbf{k} = \frac{2\pi}{\lambda}\hat{k} = \frac{2\pi}{\lambda}[\sin(\theta)\cos(\varphi), \sin(\theta)\sin(\varphi), \cos(\theta)]$$

$$(3)$$

For the input field with polarization P, the intensity of E0 field is equal to:

$$\mathbf{E}_0 = [\sin(\theta - \frac{\pi}{2}).\cos(\varphi), \sin(\theta - \frac{\pi}{2}).\sin(\varphi), \cos(\theta - \frac{\pi}{2})] \qquad (4)$$

We also have S for polarization field:

$$\mathbf{E}_0 = [\cos(\phi + \frac{\pi}{2}), \sin(\phi + \frac{\pi}{2}), 0] \qquad (5)$$

When a field is applied to a particle, the polarization coefficient α is equal to:

$$\alpha_s = V\varepsilon_0 \frac{\varepsilon_r - 1}{1 + L_1(\varepsilon_r - 1)} \qquad (6)$$

In this context, $\varepsilon_r = \varepsilon_{particle}/\varepsilon_{medium}$, ε_0 is the passage coefficient of free space. Also, V is the volume of the nanoparticle and L_1 is the shape factor. For spherical nanoparticles, the shape coefficient is calculated according to the values of a, b, c as follows:

$$e^2 = 1 - \frac{b^2}{a^2} \qquad , f^2 = \frac{b^2}{a^2} - 1$$

$$L_1 = \frac{1+f^2}{f^2}[1 - \frac{1}{f}\tan^{-1}(f)] \qquad oblate\ (a < b)$$

$$L_1 = \frac{1-e^2}{e^2}(-1 + \frac{1}{2e}\ln\frac{1+e}{1-e}) \qquad prolate\ (a > b)$$

$$(7)$$

Now we can define the electric bipolar vector for each nanoparticle as follows:

$$\mathbf{P}_s = \varepsilon_0\alpha_s\mathbf{E}_{Loc}(\mathbf{r}_s) \qquad (8)$$

In this context, Ps is the induced dipole moment and E is the electric field of each nanoparticle. Thus, the field within each nanoparticle depends on two factors. An input field and the second field caused by the radiation of other nanoparticles.

The sum of these two fields makes up each nanoparticle, which is calculated from the following equation: [9]

$$\mathbf{E}_{loc,s} = \mathbf{E}_{inc,s} + \mathbf{E}_{dip,s} = \mathbf{E}_0 e^{j\mathbf{kr}_s} - \sum_{s \neq h}\mathbf{A}_{s,h}\mathbf{P}_s \qquad (9)$$

In this respect, P_s is the same as the dipole moment induced in s. Also, As, h is a 3×3 matrix that is calculated as follows.

$$\begin{cases} \mathbf{A}_{s,h} = \frac{\exp(j\mathbf{kr}_{s,h})}{\mathbf{r}_{s,h}}[k^2(r_{sh}r_{sh} - \mathbf{I}_{3\times3}) + \frac{jk r_{sh} - 1}{\mathbf{r}_{sh}^2}(3r_{sh}r_{sh} - \mathbf{I}_{3\times3})] \quad s \neq h \\ \mathbf{A}_{s,s} = \frac{1}{\alpha_s\varepsilon_0\mathbf{I}_{3\times3}} \end{cases}$$

$$(10)$$

The third step is to solve the equation and calculate the vector P from it. In this case, A is a 3N × 3N tensor. The scheme of the matrix A is shown in Fig. 4.

Fig. 4. Schematic of matrix A

In the fourth step, calculate the absorption (scattering) and scattering (extinction) properties as follows.

$$Q_{ext} = \frac{k}{\pi a^2 \varepsilon_0 \left| \overline{E}_{inc} \right|^2} \sum_{i=1}^{N} \mathrm{Im}(\overline{E}_{inc,i}^* . \overline{P}_i) \quad (11)$$

$$Q_{sca} = \frac{k^4}{6\pi^2 a^2 \varepsilon_0^2 \left| \overline{E}_{inc} \right|^2} \sum_{i=1}^{N} \left| \overline{E}_{inc,i}^* . \overline{P}_i \right|^2 \quad (12)$$

$$Q_{abs} = Q_{ext} - Q_{sca} \quad (13)$$

3. Results and discussion

Fig. 5 shows the electric field profile of a solar cell without (a) and with (b) window shape doping. It can be seen that the irregularly shaped window profile changes the field profile, which increases the photon confinement in the center of the active region.

(a)   (b)
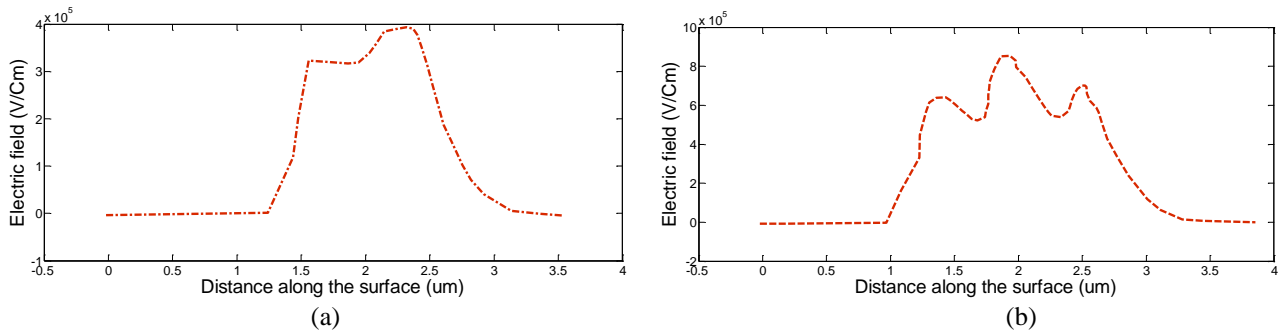
Fig. 5. The electric field profile of solar cell without (a) and with (b) window shape doping

The interaction of these photons with the nanoparticles in this region further increases the field strength and thus the power of the solar cell. The number, location, shape, and material of the nanoparticles have a large effect on this performance. Figs. 6 and 7 show four voltage/current and EQE plots of the proposed structure with different number of nanoparticles. It can be seen that the voltage, current and EQE of the solar cell change significantly when the number and location (profile of nanoparticles) are changed.
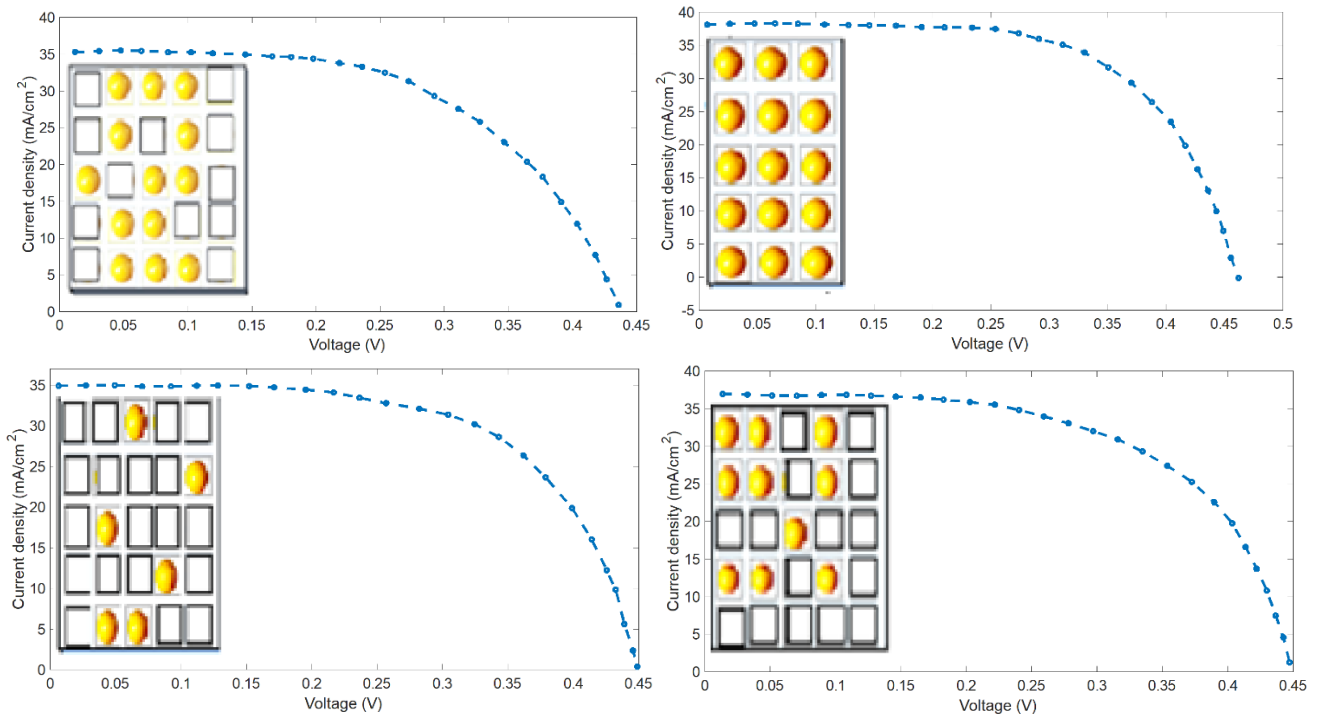
Fig. 6. Comparison of voltage-current for periodic and nonperiodic structures (color online)
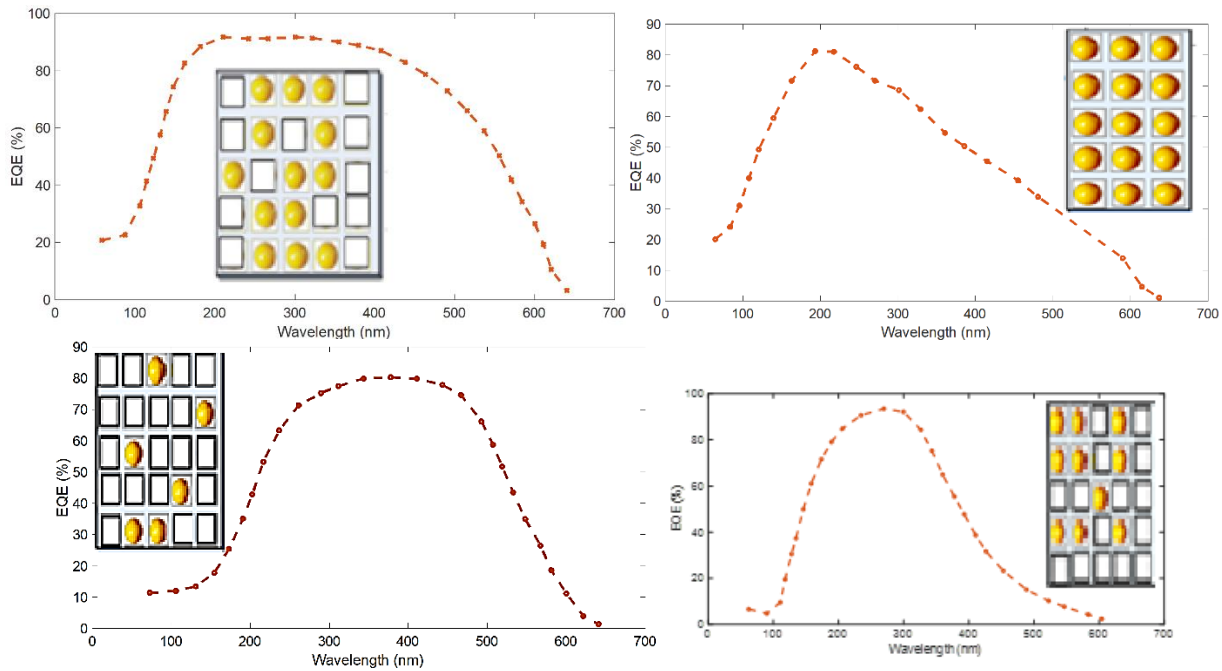
Fig. 7. Comparison of EQE for periodic and nonperiodic structures (color online)

It is well known that the maximum efficiency and current density of a solar cell change drastically depending on where and how many nanoparticles are located. Optimizing the profile of the nanoparticles could improve the performance of the solar cell.

The number, location and material of nanoparticles as well as the number of windows of doping are optimized to achieve the highest possible solar cell performance. But the size of nanoparticles is considered the same as d=20 nm. The nanoparticle structure can be optimized to achieve higher external quantum efficiency. Since the number of possible states in a 5×5 arrangement is 2^{25}=33554432, not all possible states can be considered. Therefore, we are concerned with binary optimization algorithms. One of the most famous binary optimization algorithms is the Vogel algorithm. The following is a summary of the Vogel binary algorithms.

Particle Optimization Algorithm is a search algorithm based on social exchange and behavior, which is modeled after the group behavior of weight class birds. This algorithm is an evolutionary algorithm first developed by Kennedy and Heart in 1995. The bird algorithm, like other evolutionary algorithms that do not require inference, is population-based and random. This algorithm is a mass-based algorithm that simulates the behavior of a group of birds (a group of particles) scanning various points in search of a location and pushing the group to a more hopeful point (points where the answer is likely to be reached). There are others nearby. The algorithm collects the information gathered by the particles within the group. A particle moves towards the answer space (search) according to the path of motion defined by its velocity. The velocity of each particle is determined by the personal experience of the particle and the experience of the neighboring particles. Therefore, during the search

process, particles tend to move towards better points in the response space.

The Vogel algorithm was applied to the objective function of EQE and solar cell current density, and the result can be seen in Figs. 8 and 9. The optimized nanoparticle structure is also shown in this figure.
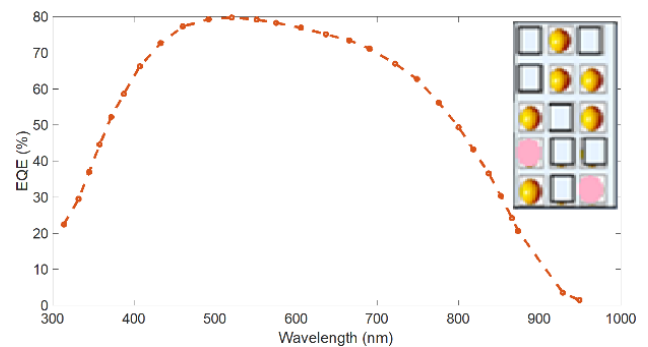
Fig. 8. The optical power of EQE for proposed structure with optimized nanoparticles (color online)
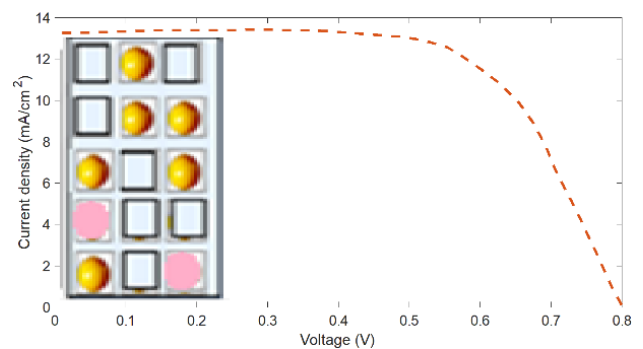
Fig. 9. The voltage-current of solar cell for proposed structure with optimized nanoparticles (color online)

Figs. 10 and 11 compare the solar cell's typical performance metrics for different periodic, non-periodic, and optimum configurations. As can be shown, non-periodic structures outperform periodic structures, and optimized non-periodic structures outperform both.
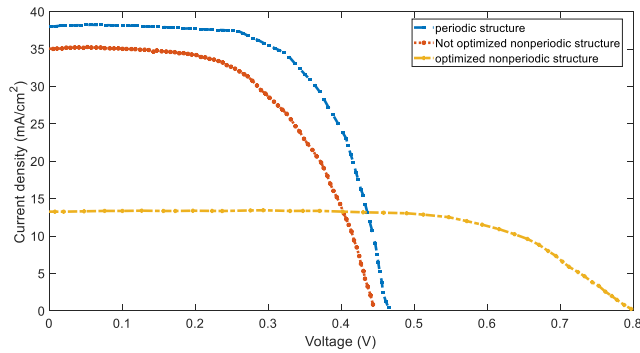
Fig. 10. Comparison of the voltage-current of solar cell for different structures (color online)
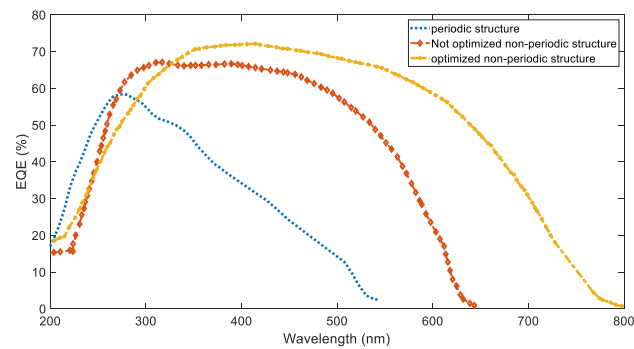
Fig. 11. Comparison of the EQE of solar cell for different structures (color online)

In the next step, we will optimize the number, depth, and duty cycle of the windowed doping. Fig. 12 shows the peak EQE of the solar cell as a function of the number of windows. It can be seen that a change in the number of windows also results in a change in EQE. With a number of 6 windows, the EQE is a maximum of 80 %.
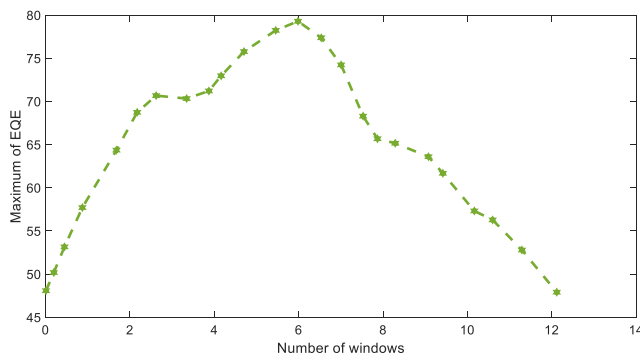
Fig. 12. The Maximum EQE as a function of the number of windows

Fig. 13 shows the EQE of the solar cell as a function of window depth. As can be seen from the figure, the depth of the windows has a much stronger effect on the performance of the solar cell. The optimized depth of 62 nm is considered for the window depth, so that the EQE reaches 86 %.
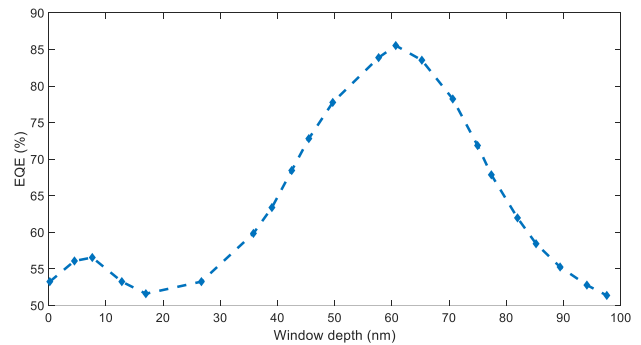
Fig. 13. The maximum EQE as a function of the windows depth

Fig. 14 current-voltage curve of optimized structure of solar cell. As is clear from the figure the current density and open voltage of solar cell is improved noticeably.
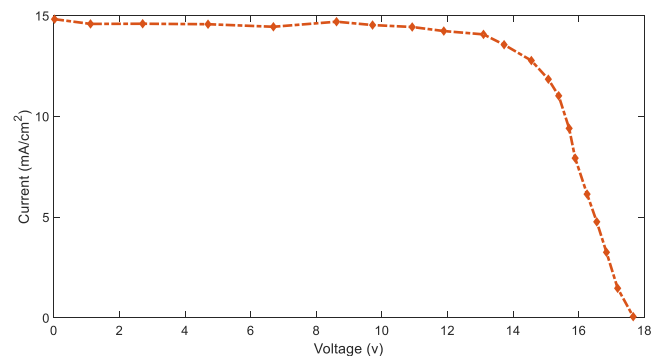
Fig. 14. current-voltage curve of optimized proposed solar cell

Another advantage of the proposed arrangement of nanoparticles is shown by the improvement of the fill factor FF for the cells, indicating the reduction of the surface resistance. This effect is expected for all solar cells that form an ohmic contact between the nanoparticle array and the cell window layer. This suggests, for example, that plasmonic nanoparticles could also be used in optically thick cells as transparent conductors to increase the FF - and thus the cell efficiency for thin, lightly doped upper window layers, although they do not increase the photocurrent. Thus, the proposed structure with window-shaped doping and nanoparticles based on the proposed profile has much higher FF and efficiency. Table 1 compares the parameters of the conventional and optimized structure of the solar cell.

Table 1. Comparison between Conventional and
the proposed structures

Structure	J_{sc}	V_{oc}	FF	efficiency
Conventional	10	0.75	0.65	10.2%
Optimized	15	0.8	0.9	18%

Therefore, with the proposed optimal structure, we improved the solar cell efficiency by more than 1.5 times. The results show that the proposed optimal structure has significantly improved the FF, EQE and efficiency of the solar cell.

4. Conclusions

In this paper, we proposed a new and optimal structure for the plasmonic solar cell such that the EQE, current density and efficiency of the solar cell are greatly improved. The proposed structure consists of a window-shaped doping and an array of plasmonic nanoparticles. In addition, a series of spherical and elliptical nanoparticles of gold or silver were added in the middle of the layer. It has been shown that by adding nanoparticles with the proposed shape, the field strength in the active region is greatly improved, leading to a significant improvement in solar cell performance. For this purpose, we use spherical and elliptical plasmonic nanoparticles of gold and silver. The number, location and material of the nanoparticles as well as the number of doping windows are optimized to achieve the highest possible solar cell performance. The simulation results show that the EQE and the light and dark current are significantly improved by the windowed doping together with optimized plasmonic nanoparticles. With the proposed optimal structure, we could improve the solar cell efficiency by more than 1.5 times. The results show that the proposed optimal structure has significantly improved the FF, EQE and efficiency of the solar cell.

References

[1] K. Benjamin, 22nd Annual Microelectronic Engineering Conference **1**, 94 (2004).
[2] H. R. Stuart, D. G. Hall, Appl. Phys. Lett. **73**, 3815 (1998).
[3] D. M. Schaadt, B. Feng, E. T. Yu, Appl. Phys. Lett. **86**, 063106 (2005).
[4] S. Pillai, K. R. Catchpole, T. Trupke, M. A. Green, J. Appl. Phys. **101**, 093105 (2007).
[5] B. P. Rand, P. Peumans, S. R. Forrest, J. Appl. Phys. **96**, 7519 (2004).
[6] C. F. Bohren, D. R. Huffman, Absorption and Scattering of Light by Small Particles Wiley, New York, 1983.
[7] H. Masuda, M. Satoh, Jpn. J. Appl. Phys., Part 2 35, L126 (1996).
[8] M. L. Brongersma, Y. Cui, S. Fan, Nat. Mater. **13**, 451 (2014).

[9] V. E. Ferry, M. A. Verschuuren, H. B. T. Li, R. E. I. Schropp, H. A. Atwater, A. Polman, Appl. Phys. Lett. **95**, 183503 (2009).
[10] F. J. Beck, S. Mokkapati, K. R. Catchpole, Prog. Photovolt. Res. Appl. **18**, 500 (2010).
[11] Z. Ouyang, S. Pillai, F. J. Beck, O. Kunz, S. Varlamov, K. R. Catchpole, P. Campbell, M. A. Green, Appl. Phys. Lett. **96**, 261109.1 (2010).
[12] X. Chen, B. H. Jia, J. K. Saha, B. Y. Cai, N. Stokes, Q. Qiao, Y. Q. Wang, Z. R. Shi, M. Gu, Nano Lett. **12**, 2187 (2012).
[13] N. Fahim, Z. Ouyang, Y. N. Zhang, B. Jia, Z. R. Shi, M. Gu, Opt. Mater. Express **2**, 190 (2012).
[14] Y. N. Zhang, Z. Ouyang, N. Stokes, B. H. Jia, Z. R. Shi, M. Gu, Appl. Phys. Lett. **100**, 151101.1 (2012).
[15] D. M. Schaadt, B. Feng, E. T. Yu, Appl. Phys. Lett. **86**, 063106.1 (2005).
[16] D. Derkacs, S. H. Lim, P. Matheu, W. Mar, E. T. Yu, Appl. Phys. Lett. **89**, 093103.1 (2006).
[17] J. L. Wu, F. C. Chen, Y. S. Hsiao, F. C. Chien, P. L. Chen, C. H. Kuo, M. H. Huang, C. S. Hsu, ACS Nano **5**, 959 (2011).
[18] N. F. Fahim, B. H. Jia, Z. R. Shi, M. Gu, Opt. Express **20**, A694 (2012).
[19] V. E. Ferry, M. A. Verschuuren, M. C. Van Lare, R. E. I. Schropp, H. A. Atwater, A. Polman, Nano Lett. **11**, 4239 (2011).
[20] T. L. Temple, G. D. K. Mahanama, H. S. Reehal, D. M. Bagnall, Sol. Energy Mater. Sol. Cells **93**, 1978 (2009).
[21] N. Fahim, Z. Ouyang, B. Jia, Y. Zhang, Z. Shi, M. Gu, Appl. Phys. Lett. **101**, 261102 (2012).
[22] B. Cai, N. Stokes, B. Jia, M. Gu, Appl. Phys. Lett. **102**, 093107 (2013).
[23] W. Yan, N. Stokes, B. Jia, M. Gu, Opt. Lett. **15**, 395 (2013).
[24] X. Chen, B. H. Jia, J. K. Saha, N. Stokes, Q. Qiao, Y. Q. Wang, Z. R. Shi, M. Gu, Opt. Mater. Express **3**, 27 (2013).
[25] N. Stokes, B. H. Jia, M. Gu, Appl. Phys. Lett. **101**, 141112.1 (2012).
[26] K. Nakayama, K. Tanabe, H. A. Atwater, Appl. Phys. Lett. **93**, 121904 (2008).
[27] S. Pillai, K. R. Catchpole, T. Trupke, M. A. Green, J. Appl. Phys. **101**, 093105 (2007).
[28] F. J. Beck, A. Polman, K. R. Catchpole, J. Appl. Phys. **105**, 114310 (2009).
[29] S. S. Kim, S. I. Na, J. Jo, D. Y. Kim, Y. C. Nah, Appl. Phys. Lett. **93**, 073307 (2008).
[30] Y. A. Akimov, W. S. Koh, Nanotechnology **21**, 235201 (2010).
[31] Z. Sun, X. Zuo, Y. Yang, Opt. Lett. **37**, 641 (2012).
[32] V. E. Ferry, L. A. Sweatlock, D. Pacifici, H. A. Atwater, Nano Lett. **8**, 4391 (2008).
[33] P. Berini, Phys. Rev. B **63**, 125417 (2001).
[34] V. Giannini, Y. Zhang, M. Forcales, J. Gómez Rivas, Opt. Express **16**, 19674 (2008).
[35] F. J. Haug, T. Söderström, O. Cubero, V. Terrazzoni-Daudrix, C. Ballif, J. Appl. Phys. **104**, 064509 (2008).

[36] R. B. Konda, R. Mundle, H. Mustafa, O. Bamiduro, A. K. Pradhana, U. N. Roy, Y. Cui, A. Burger, Appl. Phys. Lett. **91**, 191111 (2007).

[37] J. Weickert, R. B. Dunbar, H. C. Hesse, W. Wiedemann, L. Schmidt-Mende, Adv. Mater. **23**, 1810 (2011).

[38] L. Lu, Z. Luo, T. Xu, L. Yu, Nano Lett. **13**, 59 (2013).

[39] W. Zhang, M. Saliba, S. D. Stranks, Y. Sun, X. Shi, U. Wiesner, H. J. Snaith, Nano Lett. **13**, 4505 (2013).

[40] D. M. Callahan, J. N. Munday, H. A. Atwater, Nano. Lett. **12**, 214 (2011).

[41] J. N. Munday, H. A. Atwater, Nano Lett. **11**, 2195 (2011).

[42] M. G. Deceglie, V. E. Ferry, A. P. Alivisatos, H. A. Atwater, Nano Lett. **12**, 2894 (2012).

_____
[*]Corresponding author: Donyaadabi@yahoo.com